Soil Biology and Biochemistry 147 (2020) 107836

Contents lists available at ScienceDirect

Soil Biology and Biochemistry

journal homepage: http://www.elsevier.com/locate/soilbio

Depth patterns and connections between gross nitrogen cycling and soil exoenzyme activities in three northern hardwood forests

Bridget A. Darby[a], Christine L. Goodale[a,*], Nathan A. Chin[a,b], Colin B. Fuss[a,c,d], Ashley K. Lang[c,e], Scott V. Ollinger[f], Gary M. Lovett[c]

[a] Department of Ecology and Evolutionary Biology, Cornell University, Ithaca, NY, USA, 14853
[b] Stockbridge School of Agriculture, University of Massachusetts, Amherst, MA, USA
[c] Cary Institute of Ecosystem Studies, Millbrook, NY, USA
[d] Center for Earth and Environmental Science, State University of New York - Plattsburgh, Plattsburgh, NY, USA
[e] Department of Biological Sciences, Dartmouth College, Hanover, NH, USA
[f] Earth Systems Research Center, University of New Hampshire, Durham, NH, USA

ARTICLE INFO

Keywords:
Depth patterns
Extracellular enzymes
Enzyme stoichiometry
Gross N mineralization
Nitrogen cycling
Subsoil

ABSTRACT

Despite the enormous size of the organic nitrogen (N) pool contained in mineral subsoils, rates of N cycling and soil exoenzyme activities are rarely measured in soils below 10 or 20 cm depth. Furthermore, assumed relationships between N mineralization rates and the activities of various decomposition exoenzymes are poorly characterized. We measured rates of gross and net N mineralization and nitrification as well as the potential activities of hydrolytic and oxidative enzymes at five soil depths (forest floor to 50 cm) in Spodosols at three hardwood forests of varying age (45 and 100 years post-harvest and old growth) at and near the Hubbard Brook Experimental Forest in New Hampshire, USA. As expected, rates of N cycling and potential enzyme activities per unit soil mass correlated strongly with soil carbon (C) concentration, and these parameters declined exponentially with increasing soil depth. After normalization per unit soil organic matter, N cycling rates and specific enzyme activities generally decreased little with depth within the mineral soil. Gross N mineralization rates correlated with specific activities of those enzymes that hydrolyze cellulose (β-glucosidase, cellobiohydrolase) and N-rich glucosamine polymers (N-acetylglucosaminidase), but not those that degrade protein or more complex C compounds. Hence, gross N cycling appear associated with the N released during microbial N recycling, rather than from decomposition of soil organic matter. Across the three stands, the youngest had a larger ratio of N- to-phosphorus-acquiring enzyme activities, indicating a greater N demand in younger than older forests. For all three stands, mineral soil below 10 cm contributed 30–53% of total gross and net N cycling per unit area to 50 cm depth. Overall, even though microbial N cycling and enzyme activities per unit soil mass decreased with depth, microbial processes in subsoils contributed substantially to ecosystem-scale gross N fluxes because of the sustained microbial activity per unit soil organic matter at depth and the large size of the organic matter pool in the mineral soil. These results support the inclusion of often-ignored mineral subsoils and microbial N recycling in both ecosystem N budgets and in model simulations, due to their contribution to soil N fluxes and the importance of microbial N dynamics in forest stands.

1. Introduction

Studies measuring soil microbial nitrogen (N) cycling and extracellular enzyme activity (e.g., as synthesized in Booth et al., 2005; Sinsabaugh et al., 2008) typically focus exclusively on the carbon (C)-rich forest floor (O horizon) and surface mineral layers (usually to 10 or 20 cm), where plant root density and soil organic matter (SOM) concentrations are typically greatest (Jobbagy and Jackson, 2001). Much less is known about microbial activity in deeper mineral soils, where C and N cycling rates are generally expected to be smaller due to steep decreases in organic C and N content and to expected increases in SOM stability (Taylor et al., 2002; Rumpel and Kögel-Knabner, 2011; Stone and Plante, 2015). SOM age and degree of mineral association both typically increase with soil depth (Gaudinski et al., 2000;

---

* Corresponding author.
E-mail address: clg33@cornell.edu (C.L. Goodale).

https://doi.org/10.1016/j.soilbio.2020.107836
Received 22 November 2019; Received in revised form 20 April 2020; Accepted 23 April 2020
Available online 1 May 2020

McFarlane et al., 2013; Schrumpf et al., 2013; Kramer et al., 2017; Porras et al., 2017). Existing studies of microbial processes in deep soil have found that microbial biomass, enzyme activity, and N cycling per unit soil mass decrease with depth, but are still detectable below 30 cm depth (Federer, 1983; Taylor et al., 2002; Matejek et al., 2010; Iversen et al., 2011; Herold et al., 2014; Stone et al., 2014, 2015), and can respond to perturbations by harvest (Kellman et al., 2014), priming (Bernal et al., 2016), and warming (Fierer et al., 2003; Hicks Pries et al., 2017). A global data set indicates that over 60% of soil organic N (SON) in the top meter of soil occurs below 20 cm (Jobbagy and Jackson, 2001). Consequently, when multiplied by the large size of the mineral soil pool, even small rates of microbial activity per unit soil mass at depth could contribute meaningfully to ecosystem-scale soil N cycling (Matejek et al., 2010; Iversen et al., 2011).

Gaps persist in quantifying N cycling rates and N budgets in deep soil even at well-studied sites, such as the Hubbard Brook Experimental Forest (HBEF), a Long-Term Ecological Research site in the White Mountains of New Hampshire, where the mineral soil may play a more important role than previously recognized in both supplying and retaining N over the course of succession (Lovett et al., 2018; Fuss et al., 2019). Changes in SON stocks are extremely difficult to detect because of the great size and spatial heterogeneity of this pool (e.g., Johnson, 1995). Yet at the HBEF and elsewhere, ecosystem-scale N budgets often show that trees must acquire N from the mineral soil during early decades of regrowth (e.g., Johnson, 1992; Richter et al., 2000; Compton et al., 2007; Lovett et al., 2018). They could plausibly do so by stimulating N mineralization through allocation of photosynthate to mycorrhizal symbionts (e.g., Hobbie and Hobbie, 2006; Talbot et al., 2008; Frey, 2019) and by priming of microbial decomposition activity with exuded labile C compounds (Kuzyakov et al., 2000). As plant biomass accumulation slows in mature stands, soils could then re-accumulate N that is no longer required for new plant biomass (Kaye et al., 2003; Lovett et al., 2018; Fuss et al., 2019).

Microbial processes can both add and remove N from SON pools. Microbes drive the process of N mineralization, which is the decomposition-mediated release of N from organic matter. Microbial production of a range of extracellular enzymes propels the first step of this process, the depolymerization of complex organic matter into simple monomers (Schimel and Bennett, 2004; Schmidt et al., 2011). Microbes also contribute to the production of SON through their uptake (immobilization) of N and the subsequent turnover and stabilization of microbial products (e.g., Sollins et al., 2009; Bingham and Cotrufo, 2016). Measurements of net N mineralization capture the balance between microbial production and consumption of inorganic N and are relatively simple to conduct, while ^{15}N-based measurements of gross N cycling quantify rates of both the production and the consumption of inorganic N, but are more complicated and expensive (Davidson et al., 1991; Hart et al., 1994; Robertson et al., 1999; Schimel and Bennett, 2004). Measurements of the potential activities of soil exoenzymes are increasingly used to provide information on the decomposition process (e.g., Sinsabaugh and Moorhead, 1994; Fierer et al., 2001; Schimel and Bennett, 2004; Sinsabaugh et al., 2002; Weintraub et al., 2007; Allison et al., 2008), and in construction of a new generation of SOM models (e.g., Allison et al., 2010; Wieder et al., 2013, 2015). In addition, the ratios of C-, N- and P-acquiring enzyme activities ("ecoenzymatic stoichiometry") are sometimes used to assess relative microbial nutrient limitation (e.g., Sinsabaugh et al., 2008, 2009; Sinsabaugh and Follstad Shah, 2011; Zechmeister-Boltenstern et al., 2015; Moorhead et al., 2016). Yet, although some studies report relationships between enzyme activities and rates of substrate C mineralization, few if any have demonstrated direct correspondences between enzyme activities and rates of gross or net N mineralization (Mooshammer et al., 2014). Mineralization of inorganic N might be assumed to correspond simply with the activity of the N-acquiring enzymes. Alternatively, correspondence of N mineralization with the activity of hydrolytic enzymes involved in breakdown of labile C compounds could reflect microbial dependence on the supply of these substrates, while correspondence with the activity of oxidative enzymes might reflect dependence on the release of N from more complex organic matter.

This study examined how rates of soil N cycling and potential activities of extracellular enzymes varied with each other and with depth in three forest stands of different ages at and near the HBEF, in order to quantify the contributions of mineral subsoils to ecosystem N cycling and to identify links between these N cycling rates and the activity of soil exoenzymes. Measuring both gross and net N cycling rates and a suite of potential exoenzyme activities in the same samples allowed examination of the connections between these indicators of microbial activity, both per unit soil dry mass and when normalized for SOM concentration. We hypothesized first that gross N mineralization rates would correspond with the specific activities of commonly measured soil exoenzymes, particularly those associated with N acquisition: N-acetylglucosaminidase (NAG), which hydrolyzes glucosamine from chitin and other oligosaccharides, and leucine aminopeptidase (LAP), which hydrolyzes leucine and other amino acids from polypeptides. This hypothesis addresses the expected link between activities of decomposition enzymes and N cycling, and whether mineralization of inorganic N depends more on the activity of enzymes degrading N-containing organic compounds than those degrading other types of organic matter. Second, we hypothesized that potential enzyme activities and N cycling rates per unit soil mass would both decrease with depth, because expected decreases in SOM concentrations provide less organic substrate for decomposition. In addition we expected that when normalized for SOM content, these processes would decrease with depth due to expected increases in the age and stability of the SOM that occurs in deep soil. Third, we hypothesized that potential enzyme activities and gross N mineralization rates would be greatest in the youngest site, because greater plant demand for N might lead plants to allocate C belowground to stimulate microbially driven release of N through decomposition of SOM.

2. Methods

2.1. Site description

Soils were collected in July 2014 from three sites at and near the HBEF, where monthly mean temperature is 18 °C in July and −9 °C in January, and precipitation averages 1400 mm per year. Soils are largely acidic sandy loam Spodosols derived from glacial till, and are classified as well-drained Haplorthods (Likens, 2013). Soil C stocks and the thickness of the forest floor (O horizon), eluviated (E), and spodic (Bhs and Bs) soil horizons vary with topographic position (Bailey et al., 2014), but intensive measurements in HBEF's Watershed 5 indicate that the forest floor contains, on average, 1.3 t N ha^{-1} and 30 t C ha^{-1} and the mineral soil contains another 5.9 t N ha^{-1} and 130 t C ha^{-1} to the C horizon or bedrock at about 60 cm depth (Johnson, 1995). The first site was a young stand at HBEF's Watershed 4 (W4; "young"), which was strip-cut between 1970 and 1974 and thus 40–44 years old at the time of sampling. The second site was a mature forest site west of Watershed 6 (W6; "mature"), which is the biogeochemical reference watershed at HBEF, and was heavily logged between 1906 and 1920 and thus approximately 100 years old at the time of sampling (Peart and CogbillPalmiotto, 1992). This site was located ~300 m west of the "W6 mid-elevation hardwood" long-term monitoring site described in other HBEF studies (e.g., Bohlen et al., 2001; Groffman et al., 2018). The third site was an old-growth stand located on Mt. Moosilauke (MO; "old-growth"), ~10 km northwest of the HBEF. This site has no history of forest harvest (Brown, 1958), and has been used to characterize stream NO_3^- losses from old-growth forests (Vitousek and Reiners, 1975; Goodale et al., 2003). Tree-ring measurements confirmed that canopy trees were >200 years old (Keurajian, 2015). All three sites support northern hardwood tree species, particularly sugar maple (*Acer saccharum*), which forms associations with arbuscular mycorrhizae, and yellow birch (*Betula alleghaniensis*), an ectomycorrizal tree species. The youngest site, W4, had less sugar maple than the two older sites, and instead contained another arbuscular mycorrhizal tree species, white ash *(Fraxinus americana)* (Table 1). These three sites formed part of an eight-site chronosequence (Lovett et al., 2018; Fuss et al., 2019), but the intensive measurements described here occurred only at these three focal stands, which thus lack replication by stand age and consequently provide limited evidence for examining changes in these processes over succession. Nonetheless, measurements at even a few sites can characterize changes in microbial processes with soil depth and provide useful examples of cross-site variation by soil or vegetation type (e.g., Fierer et al., 2003; McFarlane et al., 2013; Stone et al., 2014, 2015; Stone and Plante, 2014, 2015; Kramer et al., 2017; Porras et al., 2017).

2.2. *Field and laboratory methods*

At each site, eight soil cores were collected from within a 900 m^2 plot; half were randomly selected for the microbial analyses described here. The forest floor (Oe/Oa) was collected by removing loose leaf litter (Oi), then using a knife to collect a block of the Oe and Oa horizons from within a 15 × 15 cm wooden frame. A diamond bit rotary corer (Rau et al., 2011) with a 9.5 cm internal diameter enabled quantitative collection of the underlying mineral soil in 10 or 20 cm increments to 50 cm depth (0–10, 10–20, 20–30, and 30–50 cm). All analyses described here were performed on all 60 soil samples (3 sites × 4 cores per site × 5 depths per core), with minor exceptions noted below. Samples were stored on ice packs during transport and at 4 °C in the laboratory until processing. Soils were sieved within 24 h of collection using a coarse sieve (4 mm) to quickly homogenize the sample and remove large rocks and roots. Sub-samples of sieved soil were stored at −20 °C for later use in enzyme activity assays. The remaining soil was stored at 4 °C for up to 2 more days for the N cycling assays.

Bulk density and soil C and N stocks were determined from the quantitative soil samples following Rau et al. (2011). Briefly, 10 g subsamples of sieved soil were taken for moisture determination by drying for 1 day at 110 °C, and for C and N analysis after grinding to a fine powder with a ball mill (Retsch mixer mill MM200; Verder Scientific, Newtown, Pennsylvania, USA). Soil C and N concentration and isotopic composition were measured at the Cornell Stable Isotope Laboratory in Ithaca, NY, using a Finnigan MAT Delta Plus mass spectrometer following combustion with an elemental analyzer (Carlo Erba NC2500; Thermo Finnigan, San Jose, CA, USA). Surface mineral soil pH was measured with an Accumet AB15 pH meter (ThermoFisher Scientific, Waltham, MA, USA) with a 1:2 ratio of dry soil to water (Table 1).

Table 1
Location, soil pH, stand age, and relative biomass of dominant tree species at the three forest stands.

	Young Watershed 4 (W4)	Mature West of Watershed 6 (W6)	Old-Growth Mt. Moosilauke (MO)
Latitude/Longitude	N 43.95442° W 71.73004°	N 43.94960° W 71.74051°	N 44.00077° W 71.85913°
Elevation (m)	568	635	824
Soil (0–10 cm) pH ± std. dev.	3.8 ± 0.3	3.6 ± 0.01	3.8 ± 0.3
Approximate stand age (years)	40	100	>200
Fraction of tree biomass, by species			
Acer saccharum (AM)	16%	73%	72%
Fraxinus americana (AM)	24%	0%	0%
Betula alleghaniensis (ECM)	55%	17%	27%
Fagus grandifolia (ECM)	3%	10%	0%
Other species	2%	1%	1%

Tree species typically associated with arbuscular mycorrhizae (AM) or ectomycorrhizae (ECM).

2.3. *Gross and net N cycling measurements*

Rates of gross N mineralization and nitrification were assessed using the isotope pool dilution method (Davidson et al., 1991; Hart et al., 1994), in which a known amount of $^{15}NH_4^+$ or $^{15}NO_3^-$ is added to a soil sample, and its rate of dilution by mineralization or nitrification of unlabeled N is measured over 24 h. To quantify rates of gross N mineralization and $^{15}NH_4^+$ consumption, 7.53 μg N of 98 atom% $(^{15}NH_4)_2SO_4$ were added to a pair of 15 g field-moist sub-samples, each in a 125 mL HDPE bottle. The label, along with 1 mL of deionized water, was distributed within each sub-sample using a 250 μg syringe. One sub-sample from each pair was extracted with 50 mL of 2M KCl within 15 min of labeling, and the second sub-sample was extracted after incubation in the dark for 24 h at room temperature. The KCl extracts were stored in 60 mL HDPE bottles and frozen at −20 °C until chemical analysis. The same procedure was used to estimate rates of gross nitrification and $^{15}NO_3^-$ consumption in another pair of subsamples using 1.63 μg N of 98% $K^{15}NO_3^-$ per subsample. These ^{15}N additions were based on previous measurements of gross N cycling at similar northern hardwood forests (Christenson et al., 2009; Fisk et al., 2002).

The KCl extracts were analyzed with colorimetric methods for NH_4^+ (alkaline phenate) and $NO_3^- + NO_2^-$ (cadmium reduction) concentrations using a Quikchem 8100 flow injection analyzer (Lachat Instruments, Milwaukee, WI, USA) at the Cary Institute of Ecosystem Studies in Millbrook, NY. The N diffusion method (Brooks et al., 1989) was used to determine ^{15}N in the extract NH_4^+ or NO_3^-. Extracts with small concentrations of extractable NH_4^+ or NO_3^- were spiked with known amounts (50 or 100 μg N) of unlabeled NH_4^+ or NO_3^- to ensure that each sample contained sufficient N for diffusion and ^{15}N analysis. For the diffusions, two small glass fiber filters were acidified with 20 μL $KHSO_4$, then sealed in a Teflon tape packet that was floated on each KCl extract in a 125 mL HDPE bottle that was placed on a shaker table for seven days. MgO was added to all samples to increase pH and convert NH_4^+ to $NH_{3,}$ which is trapped on the acidified filters. Devarda's alloy was also added to the $^{15}NO_3^-$-labeled extracts to convert NO_3^- to NH_4^+; filters in these extracts collected both NH_4^+ and NO_3^-. Filter ^{15}N contents were analyzed at the Cornell Stable Isotope Laboratory as described above. Pre-spike $^{15}NH_4^+$ and $^{15}NO_3^-$ extract concentrations were computed using mean ^{15}N measurements of the unlabeled spike solutions, and assuming that ^{15}N values of the unlabeled NH_4^+ in the extracts for gross nitrification matched the natural abundance ^{15}N measured in corresponding soil samples (Högberg, 1997).

Gross N cycling rates were calculated using the differences in atom percent ^{15}N enrichment above background (APE) and in inorganic N concentrations between the pre- and post-incubated samples using the equation in Hart et al. (1994), originally developed by Kirkham and Bartholomew (1955):

$$m = \frac{[NH_4^+]_0 - [NH_4^+]_t}{t}{*}\ \frac{log(APE_0/APE_t)}{log([NH_4^+]_0/[NH_4^+]_t)} \tag{1}$$

$$c = m - \frac{[NH_4^+]_t - [NH_4^+]_0}{t} \tag{2}$$

where m = the gross mineralization rate, APE = the ^{15}N atom percent excess in the NH_4^+ pool, c = the gross NH_4^+ consumption rate, t = incubation time, and $[NH_4^+]$ = the total extractable NH4+-N concentration (μg N/g dry soil) at time 0 or t. Gross rates of nitrification and NO_{3-} consumption were calculated using the same equation, after replacing $[NH_4^+]$ with $[NO_{3-}]$. Lack of ^{15}N enrichment for four of the 240 diffusions prevented calculation of two each of the 60 gross mineralization and nitrification rates. One-day net N mineralization and nitrification rates were calculated using the pre- and post-incubation extractable inorganic

N measurements collected during the gross N mineralization assay. Net N mineralization was calculated as $([NH_4^+\text{-N}] + [NO_3^-\text{-N}])_{incubation}$ - $([NH_4^+\text{-N}] + [NO_3^-\text{-N}])_{initial}$ and net nitrification was calculated as $[NO_3^-\text{-N}]_{incubation}$ - $[NO_3^-\text{-N}]_{initial}$.

2.4. *Extracellular enzyme potential activities*

Two soil slurries were created for each soil sample, each using 2 g of soil in 150 mL of a 50 mM sodium acetate buffer (pH 5.0) homogenized with a hand blender. One slurry was used for measurements of hydrolytic enzyme activity and the other for oxidative enzyme activity. Lack of material precluded analysis of oxidative enzyme activity for one sample at the old-growth site and eight samples at the mature site, including all four of its forest floor samples. For both sets of enzyme analyses, 50 μL of each sample slurry was added to 8 replicate wells in a column of a 96-well plate.

Potential activities of six hydrolytic enzymes used for microbial acquisition of C-, N-, and P were quantified with fluorometric assays using the method outlined in German et al. (2011). These enzymes included two used to degrade cellulose, β-glucosidase (BG) and cellobiohydrolase (CB); one to degrade hemicellulose, β-xylosidase (BX); one to acquire phosphorus, acid phosphatase (AP); and two used to acquire N, NAG for amino sugars and LAP for amino acids. A fluorescent substrate specific to each enzyme function was added to the plate, which was then incubated in the dark at room temperature. Assays were run alongside a standard curve containing soil homogenate with an increasing concentration of methylumbelliferone (MUB), except for the LAP analyses which used amidomethylcoumarin (AMC) standards. Fluorescence was measured on a microplate reader set at 365 nm excitation and 450 nm emission, and converted to units of potential enzyme activity per unit dry mass (nmol g^{-1} h^{-1}) as in German et al. (2011).

Potential activity of the lignolytic oxidative enzyme phenol oxidase (POX) was assessed using two different enzyme substrates, ABTS (2,20-azino-bis(3-ethylbenzthiazoline-6-sulfonic acid)) and L-DOPA (L-3,4-dihydroxyphenylalanine), as suggested by Bach et al. (2013) on account of the variability of these assays. These activities are referred to here as POX_{ABTS} and POX_{LDOPA}, respectively. Plates were incubated in the dark for 24 h at room temperature after adding the L-DOPA or ABTS substrates. Before measurement, 150 μL of each well was transferred onto a clear reading plate with transparent well bottoms. The same storage and slurry preparation methods were used for assessing potential activities of hydrolytic and oxidative enzymes, but any disproportional effects of these methods on larger fungi (e.g. homogenization) are more likely to affect oxidative than hydrolytic enzyme activities.

Enzyme assays were all conducted on soil samples stored by freezing at −20 °C. This commonly used storage method (e.g., Stone et al., 2014; Fatemi et al., 2016; Riggs and Hobbie, 2016; Baker and Allison, 2017; Looby and Treseder, 2018) is recommended for when these assays cannot be conducted within a few days of collection (e.g., Robertson et al., 1999; Lee et al., 2007; DeForest, 2009; Wallenius et al., 2010; Bach et al., 2013). Methods comparisons show that freezing has little influence on enzyme activities relative to analyses of fresh samples for soils spanning a range of SOM concentrations (Lee et al., 2007; Wallenius et al., 2010). A study from acidic deciduous forests similar to HBEF found that storage by freezing increased variability in NAG, AP, and POX_{LDOPA} activities but had little effect on BG, BX, and peroxidase activities (DeForest, 2009). Thus, values in this study represent relative indices of potential enzyme activity across samples rather than absolute quantities, and could possibly include intracellular activity released by cell lysis from freezing. Any relationships that emerge between enzyme activities and sample depth or N cycling rates occur in the context of potential variability induced by storage by sample freezing.

2.5. *Statistical analysis*

Nitrogen cycling measurements were examined per unit dry soil mass (μg N g^{-1} soil d^{-1}), normalized per unit soil N or C (g N kg^{-1} N or g N kg^{-1} C d^{-1}), and on an areal basis (kg N ha^{-1} d^{-1}). Enzyme activities were examined as both activity per unit soil dry mass (nmol g^{-1} soil h^{-1}) and as specific activity normalized per unit soil C (μmol g^{-1} C h^{-1}) (e.g., Sinsabaugh et al., 2008; Sinsabaugh and Follstad Shah, 2011; Stone et al., 2014). Enzymatic C- to N and N-to P acquisition ratios were computed as ln(BG) : ln(NAG + LAP) and ln(NAG + LAP) : ln(AP), respectively, as presented by Sinsabaugh et al. (2008). The ratio of ln (BG) : ln(POX) was also computed as an index of the relative abundance of labile to recalcitrant C (Sinsabaugh and Follstad Shah, 2011). Two-way ANOVA was used to determine statistically significant ($P < 0.05$) differences in N-cycling rates and enzyme activities by depth and site, and Tukey's tests were used for post-hoc comparisons. Strength of pairwise relationships between variables were assessed using Pearsons' correlation coefficients (R) with Bonferroni corrections for multiple comparisons, as well as corresponding coefficients of determination (R^2). Stepwise multiple linear regression was used to assess whether gross N mineralization rates were better predicted by activities of several enzymes together rather than any one enzyme alone.

3. Results

3.1. *Soil properties*

Soil C and N concentrations decreased exponentially with depth (Fig. 1 a, b), and correlated very strongly with each other across all samples ($R^2 = 0.99$; $P < 0.0001$). The forest floor had significantly greater C and N concentrations than all of the mineral soil depths, and N concentrations in the surface mineral soils (0–10 cm) were significantly greater than in deeper soils for all sites. The three sites did not differ significantly from each other in either C or N concentration at any depth. However, the old-growth site MO had the smallest C:N ratio (<18) at all depths and the mature site W6 had the largest (≥20) with the young site W4 intermediate, although this difference was statistically significant within depth only for the two deepest layers (20–30 and 30–50 cm) (Fig. 1c). At all sites, soil C:N ratio declined from the organic horizon to 0–10 cm. Soil C:N ratio then increased between 0–10 cm and deeper soils at the two older sites but not at the young site W4.

3.2. *Nitrogen cycling rates*

When considered per unit dry soil, rates of gross N mineralization (Fig. 2a) and nitrification both varied with soil C concentrations, with stronger relationships for gross N mineralization ($R^2 = 0.83$, $P < 0.0001$) than gross nitrification ($R^2 = 0.60$, $P < 0.0001$). Rates of NH_4^+ and NO_3^- consumption (not shown) closely followed their corresponding rates of gross production (NH_4^+ $R^2 = 0.97$, $P < 0.0001$; NO_3^- $R^2 = 0.71$, $P < 0.0001$). At all three sites, gross and net N mineralization and nitrification rates all decreased significantly between the organic horizon and surface (0–10 cm) mineral soil, but did not significantly change further with increasing depth; nor did these four rates differ significantly across sites at any depth (not shown).

When computed per unit SON to normalize for potential substrate availability, gross N mineralization decreased non-significantly between the organic horizon and 0–10 cm depth, then decreased significantly between 0–10 cm and deeper mineral soil (10–20, 20–30, and 30–50 cm) (Fig. 3a). Gross nitrification rates did not differ among depths (Fig. 3c). Within each depth, neither gross mineralization nor gross nitrification differed significantly among the sites of different ages (Fig. 3 a, c). For net mineralization and net nitrification, the only significant differences by depth or site were that both rates were greater in the old-growth forest floor than at the other two sites or in the old-growth mineral soil (Fig. 3 b, d).

At the ecosystem scale, N cycling in the mineral soil contributed more mineralized N than the organic horizon due to the large mass of the mineral soil (Table 2). The 0–10 cm depth generally had the largest net

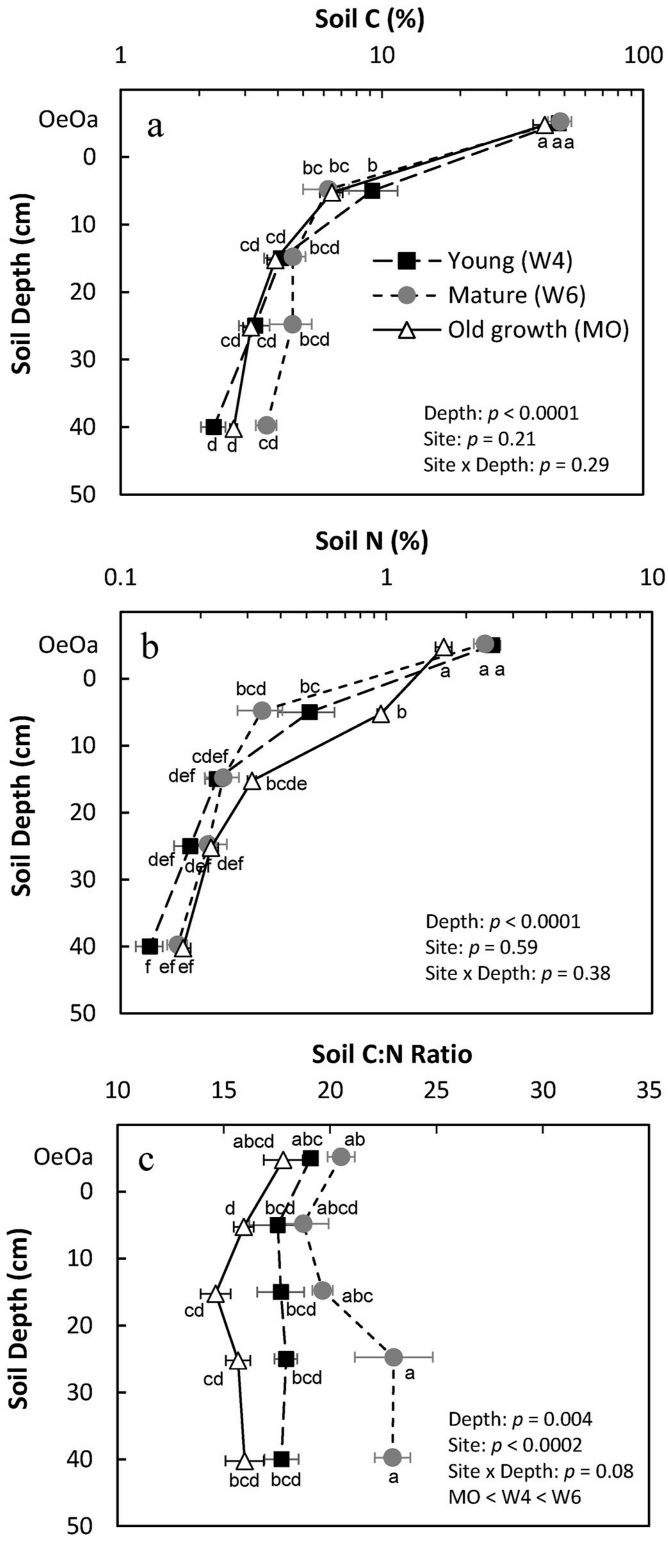

Fig. 1. Soil properties with depth for the young (W4), mature (W6), and old-growth (MO) site, including (a) soil C concentration and (b) N concentration (both log scale, % by mass), and (c) C:N ratio.

and gross N fluxes of any measured depth increment, contributing 40–46% of total N cycling on average. Nonetheless, N fluxes in soil below 10 cm contributed 30–53% of total profile N cycling to 50 cm. The only statistically significant cross-site differences among total profile gross or net N cycling rates (kg N ha^{-1} d^{-1}) were that the old-growth site had more total gross N mineralization and NH_4^+ consumption than the mature site.

3.3. Enzyme activities

Similar to depth patterns for the N cycling rates, all of the exoenzyme activities per unit soil mass declined with depth (not shown), and all increased ($P < 0.0001$) with soil C concentration (e.g., Fig. 2 b-d). Correspondence with soil C was strongest for the N-acquiring enzyme NAG ($R^2 = 0.83$; Fig. 2b) and the P-acquiring enzyme AP ($R^2 = 0.73$), and was less strong for cellulose-degrading BG ($R^2 = 0.60$; Fig. 2c) and CB ($R^2 = 0.59$), hemicellulose-degrading BX ($R^2 = 0.54$), amino acid-degrading LAP ($R^2 = 0.51$), and the two assays used for the lignolytic enzymes POX_{ABTS} ($R^2 = 0.56$; Fig. 2d) and $POX_{L\text{-}DOPA}$, ($R^2 = 0.39$). Because soil C and N concentrations covaried so strongly with each other across samples, correlations of exoenzyme activities with soil N concentrations were essentially identical as with soil C.

When normalized per unit soil C, specific enzyme activities sometimes differed between the forest floor and mineral soil, but then were remarkably constant with increased depth in the mineral soil (Fig. 4). In particular, the specific activities of the enzymes that hydrolyze glucose from cellulose (BG, CB) or glucosamine from amino sugars (NAG) sometimes decreased between the forest floor and mineral soil, in that BG specific activity at the old-growth site decreased significantly between the forest floor and deepest soil (30–50 cm); CB specific activity at the old-growth site decreased between the forest floor and all of the mineral horizons; and NAG specific activity decreased between the forest floor and mineral soil at both the mature and old-growth site, but showed more constancy with depth at the young site. By contrast, specific activities of the enzymes associated with breakdown of more complex compounds, hemicellulose (BX) and lignin and humic material (POX), sometimes increased between the forest floor and surface mineral soil, in that specific activity of BX at the young site increased significantly between the forest floor and mid-mineral soil (20–30 cm), and the specific activity of POX_{ABTS} and $POX_{L\text{-}DOPA}$ increased between the forest floor and the mineral soil at both the young and old-growth sites. (The mature site lacked POX measurements for this comparison.) Within the mineral soil, specific activity of POX was greatest in the top two mineral layers (0–10 and 10–20 cm) relative to deeper soil at all three sites.

Compared across sites, for all enzymes except NAG, the old-growth site regularly had significantly greater specific enzyme activity than the mature stand at most depths, while specific activities at the youngest site typically fell intermediate to the other two sites (Fig. 4). For NAG, however, the youngest site had greater specific activity throughout the mineral soil than the two older sites, although these differences were not statistically significant. The youngest site did have a significantly smaller enzymatic ratio of C:N-acquisition (i.e., ln(BG) : ln(NAG + LAP)) than the old-growth site and a significantly larger enzymatic N:P-acquisition ratio (i.e., ln(NAG + LAP) : ln(AP)) than both of the older sites, suggesting greater microbial N limitation relative to either C or P (Fig. 5). The ratio of ln(BG) : ln(POX_{ABTS}), indicating the ratio of labile to complex C breakdown, was significantly smaller in the mature site compared to the other two sites, with a similar trend for ln(BG):ln (POX_{LDOPA}) ($P = 0.10$).

3.4. Correspondences between enzyme activities and N cycling rates

When considered per unit soil mass, gross N mineralization rate correlated significantly ($P < 0.002$) with all enzyme activities ($R^2 = 0.87$ for NAG, 0.78 for BG, 0.76 for CB, 0.76 for LAP, 0.73 for BX, 0.38 for POX_{ABTS}, and 0.29 for POX_{LDOPA}), in part because of the strong covariation of both types of measurements with SOM concentration (e.g., Fig. 2). With all variables normalized per unit soil C, gross N mineralization rate corresponded most strongly with the specific activity of NAG ($R^2 = 0.46$; Fig. 6); however, it had similar relationships with both of the cellulose-degrading enzymes ($R^2 = 0.35$ for BG, 0.46 for CB,) (Table 3).

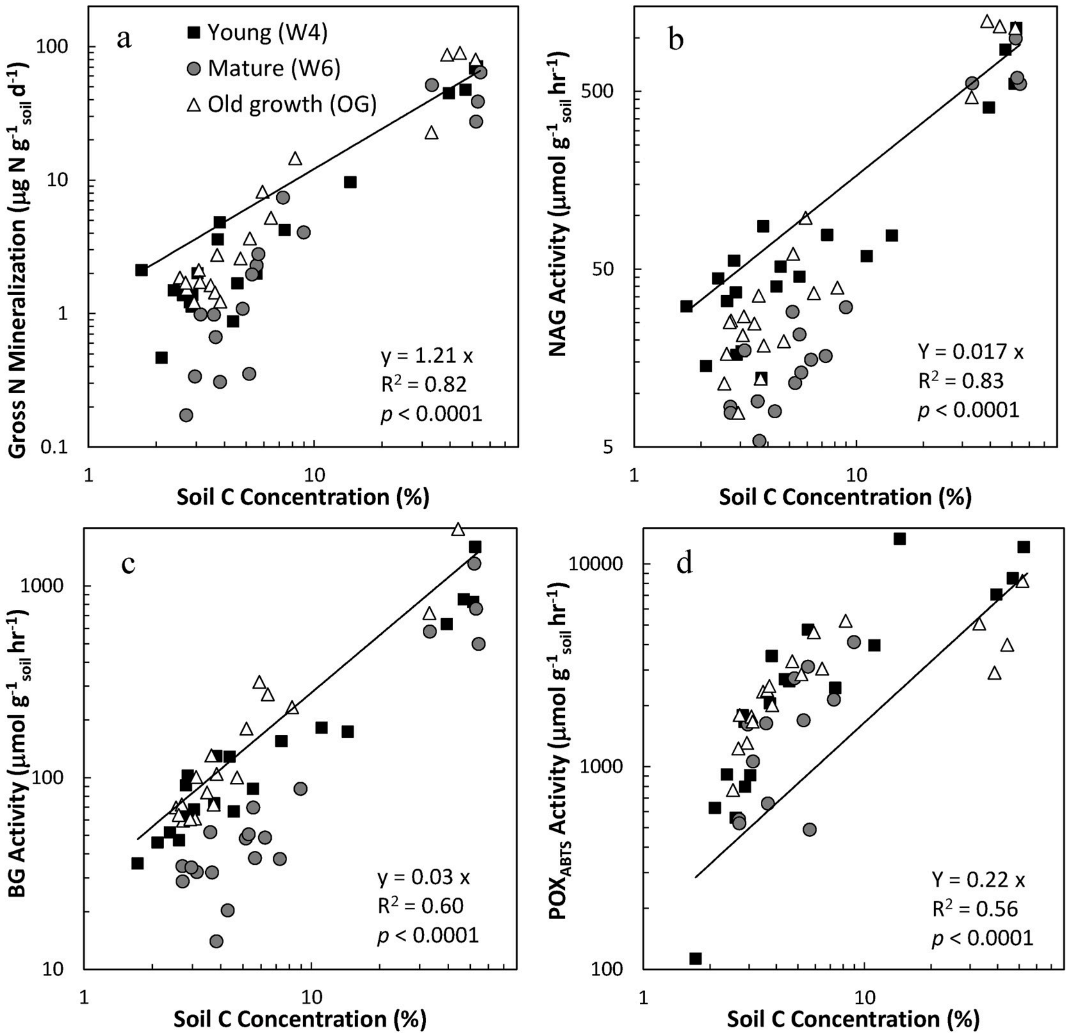

Fig. 2. Relationships between selected microbial processes and soil C concentration (%), including (a) gross N mineralization rate, (b) N- acetylglucosaminidase (NAG), (c) Beta glucosidase (BG), and (d) phenol oxidase (POX_{ABTS}), all per unit soil mass, for the young (W4, black squares), mature (W6, grey circles), and old-growth (MO, white triangles) sites.

It did not vary significantly with specific activities of LAP, BX, POX_{ABTS}, or POX_{LDOPA} ($R^2 \leq 0.11$, $P > 0.30$), nor were LAP or POX significant predictors of variation in gross N mineralization rates after accounting for variation for NAG in multiple regression analyses. Gross NH_4^+ consumption and gross nitrification rates showed similar relationships with specific activities of the same enzymes as for gross mineralization, while gross NO_3^- uptake did not vary significantly with any enzymatic measurements ($R^2 \leq 0.15$, $P > 0.07$). Net N mineralization did not vary with the specific activity of any exoenzyme except for a weak relationship with CB ($R^2 = 0.16$, $P = 0.06$). Net nitrification rate covaried with BG and CB ($R^2 = 0.32$, $P = 0.0001$) and NAG ($R^2 = 0.17$, $P = 0.04$) specific activities, similar to the gross N cycling processes.

4. Discussion

Despite the large quantities of organic C and N stored in mineral soils, few studies have measured enzyme activities or gross N cycling rates in mineral subsoils, especially when normalized for SOM content, and to our knowledge none have explored connections between these two sets of measurements. We show that N cycling rates and enzyme activities per unit soil mass decreased with increasing depth in correspondence with decreasing organic C concentration, with relatively constant rates across depths when normalized per unit soil C. We further show correlations between gross N cycling rates and the activities of those enzymes that degrade simple, but not more complex, C- and N-containing organic substrates. In the following three sections, we discuss these results and related work for each of our three hypotheses, focused on expectations that gross N mineralization rates and enzyme activities would (1) correlate with each other, particularly for the N-acquiring enzymes; (2) decrease with increasing soil depth; and (3) decrease from the young to the two older stands.

4.1. Linking N mineralization to exoenzyme activity

Nitrogen mineralization was once viewed as the relatively simple net release of inorganic N from SOM as a microbial waste product during the process of decomposition; however, conceptual models have shifted to address the earlier steps in this process, to consider depolymerization of N-containing complex organic matter and the role of microbial production of exoenzymes as drivers of decomposition (Schimel and Bennett, 2004; Schmidt et al., 2011). A new generation of SOM models now include varied representations of microbes and their decomposition enzymes (e.g., Allison et al., 2010; Wieder et al., 2013), although most major earth system models still lack explicit representation of soil microbial C–N interactions or belowground plant C allocation to these processes (e.g., Koven et al., 2013; Wieder et al., 2015). In addition, the growing field of ecological stoichiometry advances theoretical explorations of microbial C- and N- enzyme ratios during decomposition (e.g.,

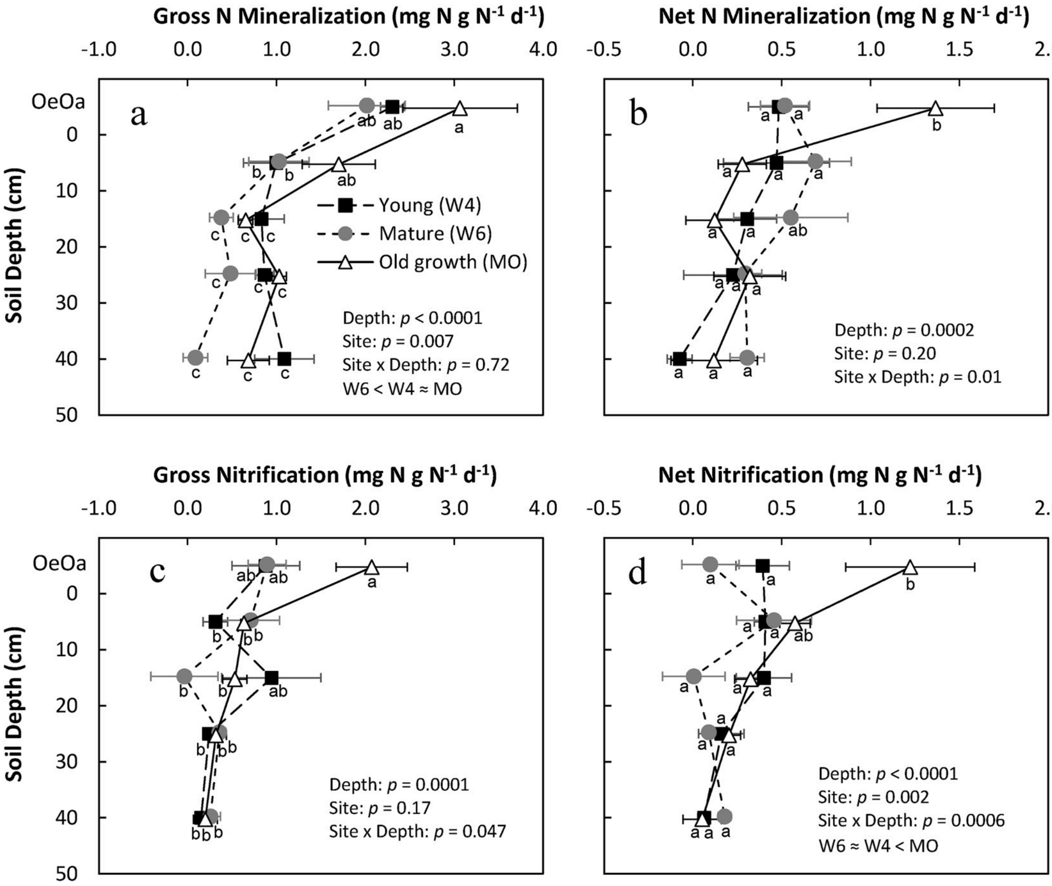

Fig. 3. Rates of (a) gross- and (b) net N mineralization and (c, d) nitrification with depth for the young (W4, squares), mature (W6, circles), and old-growth (MO, triangles) sites. Error bars represent standard errors (n = 4 per site). Different letters denote statistically significant differences ($P < 0.05$).

Sinsabaugh et al., 2008, 2009; Mooshammer et al., 2014; Zechmeister-Boltenstern et al., 2015; Moorhead et al., 2016), but studies demonstrating empirical relationships between gross N mineralization rates and the activities of decomposition exoenzymes appear to be lacking (Mooshammer et al., 2014). Of the closest such studies, one, at agricultural sites treated with dairy effluent, reported a positive relationship between gross N mineralization per unit soil mass and a different set of enzymes that target organic N compounds (deaminase, protease, and urease) (Zaman et al., 1999). Other measurements in croplands showed that cumulative net N mineralization per unit soil mass correlated positively with activities of NAG and BG, both with stronger correlations than for other N-associated enzymes (arylamidase, L-aspartase, L-asparaginase, urease, amidase, and L-glutaminase); these authors concluded that NAG activity could be a rate-limiting step in N mineralization (Ekenler and Tabatabai, 2002; Tabatabai et al., 2010).

We hypothesized that gross N mineralization rate would correspond with the activity of the enzymes generally associated with N acquisition, NAG and LAP (e.g., Sinsabaugh et al., 2008; Tabatabai et al., 2010; Sinsabaugh and Follstad Shah, 2011). The correlation observed here with NAG activity suggests a link for the enzyme-driven depolymerization of organic N to the later gross production of inorganic N. We suggest that the strong correspondences between NAG activity and gross N mineralization observed here, and by Tabatabai et al. (2010) for cumulative net N mineralization, indicate a highly labile organic substrate source for the N measured by the ^{15}N pool dilution technique, such as microbial biomass (e.g., glucosamine from chitin in fungal cell walls and peptidoglycan from bacterial cell walls) rather than N released from decomposition of more complex SOM. If so, this result supports the suggestion by Fierer et al. (2001) that microbial N recycling could explain the narrow C:N ratio of measurements of C mineralization and gross N mineralization. In their review of conceptual models of N mineralization, Schimel and Bennett (2004) noted the implication of this interpretation, that the pool dilution technique thus provides a better index of microbial N turnover than of plant-available N; they also emphasized that the ^{15}N dilution technique fails to capture earlier, often rate-limiting stages of the decomposition process in which complex polymers are broken down to easily degraded monomers. The NAG assay used here and in many other exoenzyme studies aims to capture a slightly earlier stage of the N mineralization process than methods that quantify inorganic N production, but might provide a better index of microbial N recycling than of the release of N from complex SON. Notably, the relationships between gross N mineralization and the activities of the cellulose-degrading enzymes BG and CB were nearly as strong as for NAG, indicating a strong correspondence between microbial N recycling activity and availability of cellulosic material.

Neither gross nor net N cycling rates varied significantly with the specific activities of the enzymes that degrade proteins (LAP) or lignin and humic material (POX), either directly in bivariate analyses (Table 3) or in multiple regression analyses after considering the role of NAG. LAP, BX, and especially POX all break down more complex materials than those degraded by BG, CB, and NAG, which did correlate with N cycling measurements. POX in particular is often considered important for mining N from SON (e.g., Sinsabaugh, 2010; Sinsabaugh and Follstad Shah, 2011), and its activity is frequently suppressed by experimental N fertilizations (e.g., Frey et al., 2004; Sinsabaugh et al., 2005; Weand et al., 2010; Fatemi et al., 2016; Carreiro et al., 2018). If rapid microbial turnover dominates the production of inorganic N captured by gross N mineralization measurements - as suggested above - a small, slow flux of N released from stable SON though POX activity could be too small to influence these N cycling rates or their spatial patterning through soils.

Table 2
Mean (standard error) gross and net N cycling rates, soil N pool size, and estimated turnover time by depth for the young (W4), mature (W6), and old-growth (MO) stands.

	Gross N Mineralization (kg N ha^{-1} d^{-1})			Net N Mineralization (kg N ha^{-1} d^{-1})		
Depth	W4	W6	MO	W4	W6	MO
Oe/Oa	1.0 (0.09)	1.3 (0.42)	0.9 (0.10)	0.2 (0.04)	0.3 (0.07)	0.4 (0.07)
0–10 cm	3.4 (0.28)	2.6 (0.97)	4.6 (1.26)	1.1 (0.50)	1.5 (0.21)	0.8 (0.36)
10–20 cm	1.2 (0.21)	0.8 (0.28)	1.2 (0.30)	0.4 (0.20)	1.1 (0.51)	0.1 (0.20)
20–30 cm	1.5 (0.14)	0.9 (0.52)	1.9 (0.25)	0.4 (0.33)	0.6 (0.13)	0.6 (0.44)
30–50 cm	1.8 (0.49)	0.2 (0.52)	1.8 (0.83)	−0.2 (0.37)	0.9 (0.30)	0.3 (0.44)
Total	8.8	5.6	10.1	1.5	3.8	2.3
	Gross Nitrification (kg N ha^{-1} d^{-1})			**Net Nitrification (kg N ha^{-1} d^{-1})**		
Depth	W4	W6	MO	W4	W6	MO
Oe/Oa	0.4 (0.11)	0.5 (0.14)	0.7 (0.18)	0.2 (0.04)	0.1 (0.06)	0.3 (0.07)
0–10 cm	1.1 (0.44)	2.0 (0.97)	1.7 (0.05)	1.1 (0.27)	1.1 (0.37)	1.5 (0.25)
10–20 cm	1.2 (0.52)	−0.1 (0.79)	0.9 (0.32)	0.6 (0.26)	0.0 (0.31)	0.6 (0.19)
20–30 cm	0.4 (0.09)	0.7 (0.12)	0.6 (0.25)	0.3 (0.18)	0.2 (0.06)	0.4 (0.14)
30–50 cm	0.4 (0.08)	0.8 (0.38)	0.4 (0.25)	0.2 (0.08)	0.5 (0.13)	0.1 (0.19)
Total	3.5	3.9	4.2	2.3	2.1	3.4
	N Pool Size (t N ha^{-1})			**Apparent Soil N Turnover Time (years)**[a]		
Depth	W4	W6	MO	W4	W6	MO
Oe/Oa	0.6 (0.1)	0.7 (0.2)	0.4 (0.1)	1.7	1.4	1.1
0–10 cm	2.7 (0.2)	2.4 (0.6)	2.6 (0.1)	2.2	2.6	1.6
10–20 cm	1.7 (0.2)	2.0 (0.1)	1.7 (0.4)	3.7	7.2	4.1
20–30 cm	1.8 (0.2)	2.1 (0.3)	1.8 (0.1)	3.2	6.8	2.6
30–50 cm	1.8 (0.2)	2.9 (0.3)	2.5 (0.3)	2.6	38	3.8
Total	8.6	10.1	9.0	2.6	4.9	2.4

[a] Apparent soil N turnover time calculated as pool size divided by gross N mineralization flux.

As a caveat, these inferences are derived from correlational analyses across several sites and soil depth rather than mechanistic studies. Although normalized for SOM content, both N cycling and enzyme activities could plausibly both reflect covariation with other unmeasured soil properties that underlie some of these relationships. These interpretations should be confirmed with experiments, but do broadly conform with experimental additions of extracellular enzymes to the Duke Forest, North Carolina, that showed that additions of NAG and BG enhanced net N mineralization, but addition of POX did not (Meier et al., 2017).

4.2. Microbial processes throughout soil profiles: controls, patterns, and importance

We hypothesized that soil N cycling rates and enzyme activities would decrease with depth, both because soil C and N concentrations typically decrease with depth, and because the SOM that does occur is typically older and more likely to occur in stabilized forms in association with soil minerals than at the surface (e.g., Gaudinski et al., 2000; McFarlane et al., 2013; Schrumpf et al., 2013; Porras et al., 2017). As discussed further below, we found that as expected, both gross N cycling rates and activities of all exoenzymes per unit soil mass decreased with depth corresponding with decreases in soil C concentration (Figs. 1 and 2); however, after normalizing for these changes in soil C quantity, neither set of measurements decreased greatly with depth below the forest floor (Figs. 3 and 4).

4.2.1. Soil organic matter content as a control on microbial processes

Past cross-biome data syntheses show that variation in SOM concentration in surface soils acts as a fundamental control on microbial processes measured per unit soil mass, explaining 42% of the variation of gross N mineralization (Booth et al., 2005), and 42–60% of the variance in BG, CB, NAG and AP activities (Sinsabaugh et al., 2008). The latter analysis did not include BX, and noted the lack of correspondence between SOM concentration and LAP, POX, and peroxidase activities. Measurements here illustrate the broad importance of SOM concentration over soil depths as an important control on all of these microbial processes per unit soil mass, in that variation in soil C concentration explained 60–83% of the variance in gross N cycling rates and 59–83% of the variance in BG, CB, AP, and NAG activity, as well as 51% and 39–56% of the variance in LAP and POX enzyme activities (e.g., Fig. 2). The stronger correlations with soil C in this study compared to the global syntheses likely result from the relative constancy of climate and vegetation type and wide range of soil C concentrations within our samples.

4.2.2. Patterns and importance of N cycling in mineral subsoils

Organic horizon and surface (0–10 cm) mineral soil gross and net N cycling rates measured here were broadly similar to those previously measured at the HBEF (Bohlen et al., 2001; Groffman et al., 2006, 2018) and at similar hardwood sites in the northeastern U.S. (Fisk et al., 2002; Christenson et al., 2009). Relatively few other studies of forest N cycling report measurements from deep soils. Recently, measurements from watershed 3 at the HBEF showed that rates per unit soil mass of potential C mineralization, net N mineralization, and net nitrification all decreased from Oie to Oa/A to B horizons, and correlated with variations in soil C concentration (Morse et al., 2014). Earlier measurements in three stands in New England (Federer, 1983) and in ten Norway spruce stands in Scandinavia (Persson and Wirén, 1995) showed that N mineralization rates generally decreased between the forest floor and surface mineral soil, both per unit soil mass and per unit SOM, with only small additional decreases in rates per unit SOM in deeper mineral soils, consistent with our results. Measurements of gross N cycling in deep soils are even more scarce than for net N cycling, but three studies in forests all show that gross N mineralization rates per unit soil decrease between shallow and deep mineral soils: in a red spruce chronosequence in Nova Scotia (Kellman et al., 2014), in an N-saturated Norway spruce stand in Germany (Matejek et al., 2010), and in a hardwood stand in Tennessee (Iversen et al., 2011). None of these gross N mineralization studies report rates normalized per unit SOM, soil C, or soil N. Normalizing the N cycling measurements in this study showed that these rates were faster in surface soil organic matter than in subsoils, but then changed little with increasing depth below 10 cm depth (Fig. 3), indicating relative constancy of microbial N turnover throughout the subsoil, despite an expected range of SOM ages.

Estimates of N cycling per unit area show that mineral soils contribute a substantial amount of N to total profile net and gross N cycling rates. For net N mineralization, mineral soil B horizons produced 14–58% of total profile rates in New England (Federer, 1983), and soils below 10 cm contributed a mean of 22% of total rates to 50 cm in Scandinavia (Persson and Wirén, 1995). For gross N mineralization, soils below 10 cm contributed roughly one-third of total rates in the German spruce stand (Matejek et al., 2010), and soils below 15 cm contributed 60% of total rates to 60 cm for the Tennessee hardwood stand (Iversen et al., 2011). Our measurements indicating that soils below 10 cm contributed 32–54% of total net and gross N mineralization to 50 cm (Table 2) are consistent with these prior estimates, and

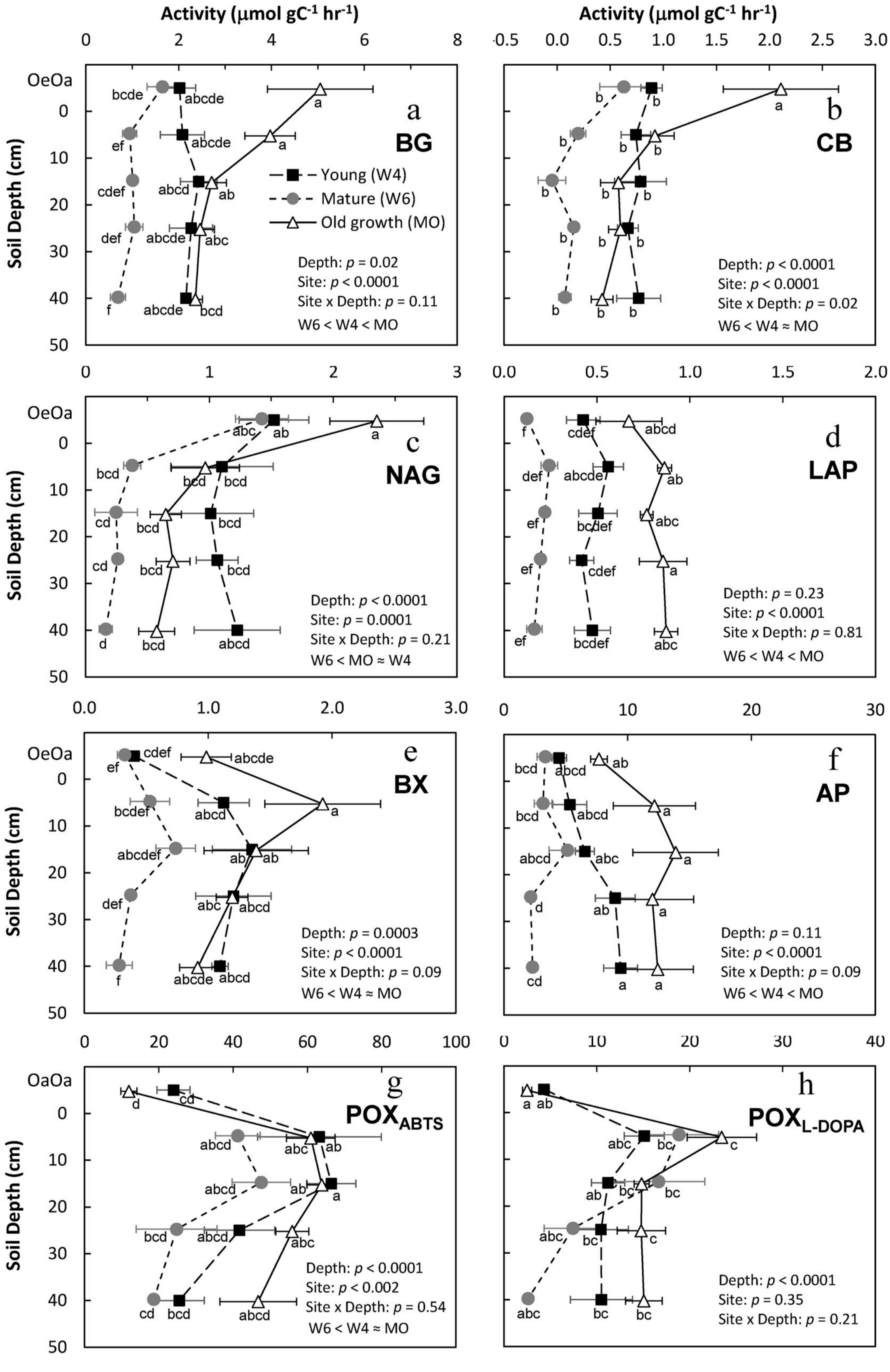

Fig. 4. Specific enzyme activity (µmol g C^{-1} hr^{-1}) with depth for the young (W4, squares), mature (W6, circles), and old-growth (MO, triangles) sites, including (a) beta glucosidase (BG), (b) cellobiohydrolase (CB), (c) N-acetylglucosaminidase (NAG), (d) leucine amino peptidase (LAP), (e) beta xylosidase (BX), (f) acid phosphatase (AP), and two assays of phenol oxidase (POX) using (g) ABTS and (h) L-DOPA substrates. Error bars represent standard errors (n = 4 at each site). Different letters denote statistically significant differences (P < 0.05).

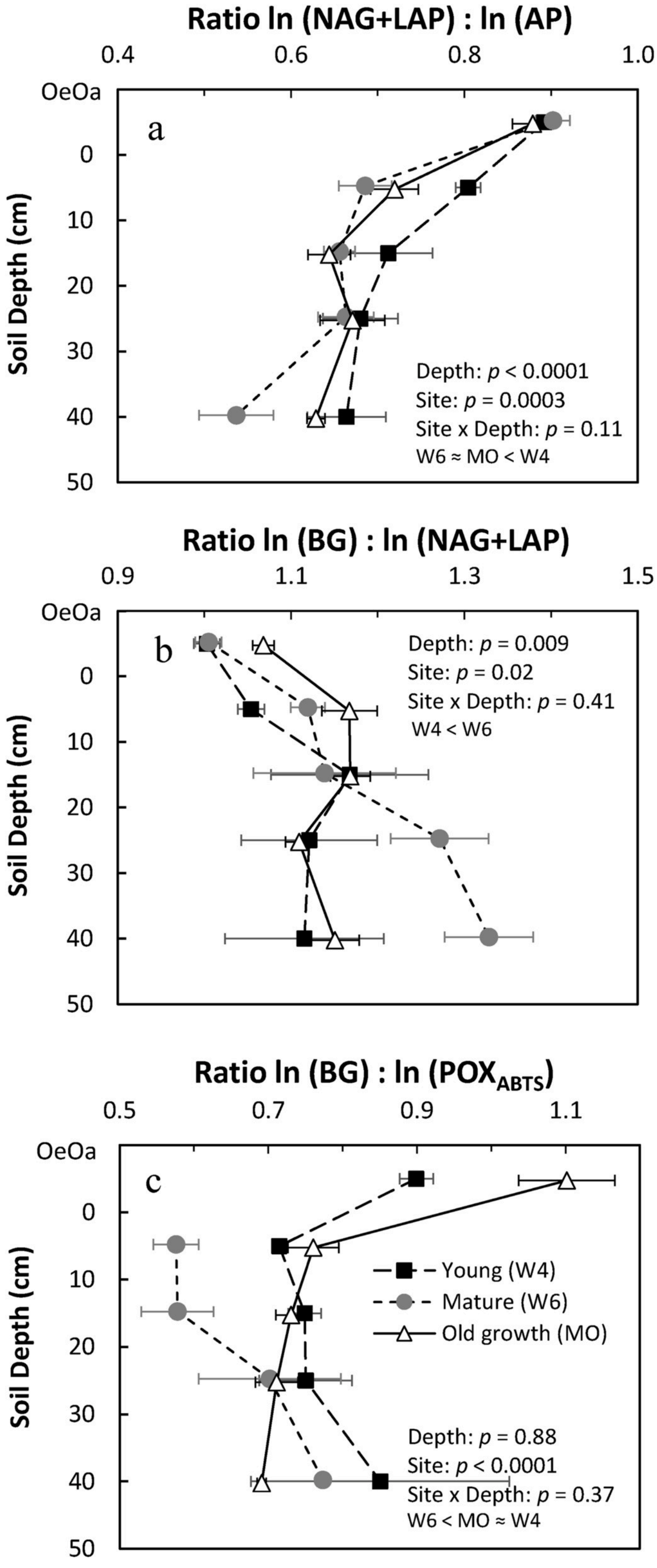

Fig. 5. Ratios of enzyme activities with depth for the young (W4, squares), mature (W6, circles), and old-growth (MO, triangles) sites, including (a) N-to P-acquiring enzymes, (b) C- to N-acquisition, and (c) labile-to complex-C degradation. Error bars represent standard errors (n = 4 at each site).

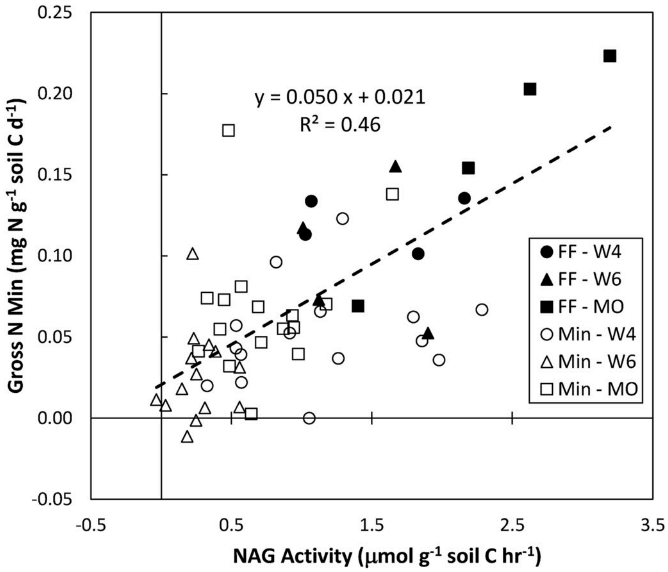

Fig. 6. Relationship between gross N mineralization and N-acetylglucosaminidase (NAG) activity, for the young (W4, squares), mature (W6, circles), and old-growth (MO, triangles) sites. Filled symbols are organic soils, open symbols are mineral soils.

illustrate the large amount of N cycling occurring in mineral subsoils.

Calculated SON turnover rates were very fast throughout the soil profile, consistent with inferences from exoenzyme activities that gross N mineralization rates better reflect microbial N turnover than new mineralization of stable SON. That is, comparison of gross N mineralization rates (kg N ha^{-1} d^{-1}) to SON stocks (kg N ha^{-1}) allows calculation of potential SON turnover times (years), as traditionally computed (pool size/flux) and conceived (i.e., mineralization as the release of N through decomposition of SON). These estimates of potential SON turnover decreased slightly with depth, from ~1 year for the forest floor to 2 years for the 0–10 cm soils and generally 3–7 years in deeper soils (Table 2) but are all very rapid. Even if mineralization activity occurred for only half the year (doubling these estimates), computed SON turnover times are still two orders of magnitude faster than ^{14}C-based measurements of SOM turnover. At nearby Bartlett Forest, a hardwood forest ~25 km from the HBEF, ^{14}C measurements indicate that mean soil C turnover time increases from ~90 years in the Oe/Oa to ~400 years at 5–15 cm to ~900 years at 30–45 cm depth (McFarlane et al., 2013). These discrepancies in apparent SOM C- and N turnover might be reconciled with the conceptual model of gross N mineralization measurements primarily reflecting the rapid and repeated microbial recycling of a small pool of labile N rather than mineralization of complex SON. If ^{14}C-based measurements best capture turnover of SOM, the comparison between ^{14}C-based estimates from Bartlett Forest and our N-flux-based turnover estimates for HBEF indicate that microbial N recycling might contribute all but a few percent of the N flux measured by the gross N mineralization measurements. Thus, earth system models that simply mineralize N along with SOM and lack this microbial N turnover (e.g., Koven et al., 2013) will greatly underestimate both ecosystem-scale gross N supply as well as the capacity for microbial N recycling.

4.2.3. *Patterns and potential controls on enzyme activity in mineral subsoils*

Of the few other studies of enzyme activity in subsoils, most report rates on a per unit soil mass basis and show that rates decline with depth, most dramatically between the forest floor and mineral soil (Taylor et al., 2002; Herold et al., 2014; Stone et al., 2014). Yet, similar to our results (Fig. 4), Stone et al. (2014) also found that specific activity per unit soil C for a set of hydrolytic enzymes remained relatively constant with increasing depth to 140 cm in a tropical forest in Puerto Rico, with

Table 3

Correlation matrix (R) among N cycling rates, soil C:N ratio, and specific enzyme activities, normalized per unit soil C.

	Gross N Min.	Gross Nitrif.	Net N Min.	Net Nitrif.	Soil C:N	BG	CB	BX	AP	NAG	LAP	POX_{ABTS}
Gross N mineralization (mg N g^{-1} C d^{-1})	1.00											
Gross Nitrification (mg N g^{-1} C d^{-1})	0.61***	1.00										
Net N mineralization (mg N g^{-1} C d^{-1})	0.50**	0.43*	1.00									
Net Nitrification (mg N g^{-1} C d^{-1})	0.51**	0.86***	0.37	1.00								
Soil C:N Ratio	−0.24	−0.12	−0.01	−0.23	1.00							
BG (μmol g C^{-1} hr^{-1})	0.59***	0.51**	0.33	0.57***	−0.46**	1.00						
CB (μmol g C^{-1} hr^{-1})	0.68***	0.57	0.40	0.57***	−0.26	0.86***	1.00					
BX (μmol g C^{-1} hr^{-1})	0.16	0.00	−0.04	0.14	−0.61***	0.63***	0.45**	1.00				
AP (μmol g C^{-1} hr^{-1})	0.05	−0.03	−0.07	0.09	−0.68**	4.00	0.25	0.67***	1.00			
NAG (μmol g C^{-1} hr^{-1})	0.68***	0.51***	0.36	0.41*	−0.24	0.70***	0.89***	0.34	0.21	1.00		
LAP (μmol g C^{-1} hr^{-1})	0.33	0.09	0.05	0.27	−0.68***	0.67***	0.49**	0.65***	0.60***	0.30	1.00	
POX_{ABTS} (μmol g C^{-1} hr^{-1})	−0.25	−0.17	−0.30	−0.04	−0.52**	0.01	−0.15	0.48*	0.35	−0.18	0.34	1.00
POX_{LDOPA} (μmol g C^{-1} hr^{-1})	−0.08	−0.20	−0.01	−0.11	−0.51**	−0.07	−0.28	0.26	0.24	−0.31	0.21	0.43*

Statistically significant correlations after Bonferroni corrections for multiple comparisons indicated as * $P < 0.05$, **$P < 0.01$, and ***$P < 0.001$.

significant decreases only for BG and NAG. They did not measure specific activity of any oxidative enzymes, which we found to peak in surface mineral soils, and to remain greater than the forest floor throughout much of the mineral soil (Fig. 4).

Why does specific enzyme activity change so little with increasing depth? Factors such as soil texture, moisture, oxygen levels, dissolved organic matter availability, and microbial community composition could all play roles affecting patterns of enzyme activity with depth, and merit further study. Stone et al. (2014) suggest that constant rates of specific enzyme activity throughout the soil profile could be due in part to constitutive enzyme activity, or the continuous microbial production of enzymes at low levels regardless of conditions (Allison et al., 2011; Sinsabaugh and Follstad Shah, 2011). They also speculate that exoenzymes could persist at depth in the Puerto Rican forest due to their stabilization on soil minerals through covalent bonding or adsorption onto soil minerals (Burns, 1982; Taylor et al., 2002), and that this stabilization decreases enzyme degradation compared to free enzymes (Ladd, 1978 ; Allison, 2006). Experiments show that addition of Al- and Fe-containing minerals to soils can increase enzyme stability and decrease their degradation (Allison, 2006), and organically complexed and poorly crystalline iron and aluminum contribute to SOC stabilization at Bartlett Forest (Porras et al., 2017) near Hubbard Brook. Subsidies of labile plant C supplied by roots and mycorrhizae could perhaps also contribute to sustaining or priming microbial production of exoenzymes and recycling of N in subsoils (e.g., Kuzyakov, 2010; Phillips et al., 2012; Schleppi et al., 2012; Bernal et al., 2016; Frey, 2019), even if much of the SOM present at depth is relatively old or stable (e.g., McFarlane et al., 2013; Schrumpf et al., 2013). Root exudates can solubilize some mineral-associated organic matter (Keiluweit et al., 2015; Yuan et al., 2018) and can also particularly stimulate the activities of NAG and BG (e.g., Meier et al., 2017), the enzymes with notably strong correspondences with gross N mineralization rates in this study (Table 3). The total annual root and rhizosphere C flux at Hubbard Brook is large, possibly more than doubling that of annual foliar production, although the exact size and depth distribution of these belowground plant C inputs are highly uncertain (Fahey et al., 2005).

4.3. Site and possible successional differences

We hypothesized that enzyme activity and gross N mineralization rates would be greatest in the youngest site (W4) as a result of priming driven by plant demand for N. However, specific oxidative and hydrolytic enzyme activities at this site typically fell intermediate between the two older sites, and rarely differed significantly among the three sites (Fig. 4). The exception to this cross-site pattern occurred for NAG activity in mineral soils (Fig. 4c), in that its activity in deeper soils at the young site often exceeded that in the older sites, and the enzymatic ratios of N- to C- and N- to P-acquisition were significantly larger at the young site than one or both of the older sites (Fig. 5). Stimulation of NAG activity relative to other enzymes could perhaps reflect increased demand for N in these young stands.

Microbial "mining" of SON has been associated with activity of POX and peroxidase, used to break down lignin and related polyphenolics (Sinsabaugh, 2010; Moorhead and Sinsabaugh, 2006; Sinsabaugh and Follstad Shah, 2011; Frey, 2019). Correspondingly, we expected the youngest stand to have the largest plant N demand and the greatest oxidative enzyme activity. However, POX specific activity in the young site was equal to or less than that of the old-growth stand. These enzymes are largely produced by saprotrophic fungi and some ectomycorrhizae, but not arbuscular mycorrhizae (Talbot et al., 2008; Sinsabaugh, 2010; Frey, 2019). Perhaps the prevalence of tree species on all three plots that form arbuscular associations (Table 1) constrained the capacity for POX production in response to plant N demand, or even shifted the plant-microbial enzymatic strategies toward priming of NAG activity rather than production of POX. In addition, with just one site for each of the stand ages, interpretations of successional drivers are limited by lack of replication, and factors other than stand age (e.g., subtle differences in soil texture, drainage, pH, or parent material) could also contribute to site-to-site differences in potential enzyme activities.

5. Conclusions

Results from this study demonstrate the often-underappreciated importance of microbial activity and N cycling in deep soils. Soil N cycling rates per unit soil mass decreased with increasing depth, but these decreases were more than compensated by the large size of the subsoil pool to contribute to ecosystem-scale N fluxes. Apparent SON turnover was rapid throughout the soil profile, and gross N cycling rates corresponded most strongly with activities of those enzymes involved in breaking down labile organic matter (NAG, BG, CB), patterns more consistent with microbial turnover and N recycling rather than N mineralization from complex SOM. Belowground plant C inputs might support these processes, and should be measured across soil depths. These observations illustrate how stand-level N budgets that neglect measurements from subsoils will greatly underestimate whole-ecosystem soil N fluxes. Decomposition models that assume that microbial activity slows with depth, or that neglect microbial N recycling, will likely to underestimate the role of soils and soil microbes as sources and sinks for N.

Declaration of competing interest

The authors declare that they have no known competing financial interests or personal relationships that could have appeared to influence the work reported in this paper.

Acknowledgments

We thank Aubree Keurajian and Liza Tetley for field assistance, Guinevere Fredriksen, Anthony Stewart, Charlotte Levy, and Bhavya Sridhar for assistance in the lab, and Tim Fahey, Dan Buckley, and Will Wieder for comments on earlier versions of this manuscript. The United States National Science Foundation provided funding, through its Division of Environmental Biology programs in Ecosystem Studies (DEB 1257808) and Long-Term Ecological Research (DEB 1114804 and 1637685), and the Division of Graduate Education programs in Integrated Graduate Education Research and Training (DGE 1069193) and Graduate Research Fellowships. Hubbard Brook is an NSF-supported Long-term Ecological Research site, and the HBEF is administered by the USDA Forest Service, Northern Research Station.

References

Allison, S.D., 2006. Soil minerals and humic acids alter enzyme stability: implications for ecosystem processes. Biogeochemistry 81, 361–373.

Allison, S.D., Czimczik, C.I., Treseder, K.K., 2008. Microbial activity and soil respiration under nitrogen addition in Alaskan boreal forest. Global Change Biology 14, 1156–1168.

Allison, S.D., Wallenstein, M.D., Bradford, M.A., 2010. Soil-carbon response to warming dependent on microbial physiology. Nature Geoscience 3, 336–340.

Allison, S.D., Weintraub, M.N., Gartner, T.B., Waldrop, M.P., 2011. Evolutionary-economic principles as regulators of soil enzyme production and ecosystem function. In: Shukla, G.C., Varma, A. (Eds.), Soil Enzymology. Springer-Verlag, Berlin Heidelberg, pp. 229–243.

Bach, C.E., Warnock, D.D., Van Horn, D.J., Weintraub, M.N., Sinsabaugh, R.L., Allison, S. D., German, D.P., 2013. Measuring phenol oxidase and peroxidase activities with pyrogallol, L-DOPA, and ABTS: effect of assay conditions and soil type. Soil Biology and Biochemistry 67, 183–191.

Bailey, S.W., Brousseau, P.A., McGuire, K.J., Ross, D.S., 2014. Influence of landscape position and transient water table on soil development and carbon distribution in a steep, headwater catchment. Geoderma 226–227, 279–289.

Baker, N.R., Allison, S.D., 2017. Extracellular enzyme kinetics and thermodynamics along a climate gradient in southern California. Soil Biology and Biochemistry 114, 82–92.

Bernal, B., McKinley, D.C., Hungate, B.A., White, P.M., Mozdzer, T.J., Megonigal, J.P., 2016. Limits to soil carbon stability: deep, ancient soil carbon decomposition stimulated by new labile organic inputs. Soil Biology and Biochemistry 98, 85–94.

Bingham, A.H., Cotrufo, M.F., 2016. Organic nitrogen storage in mineral soil: implications for policy and management. The Science of the Total Environment 551–552, 116–126.

Bohlen, P.J., Groffman, P.M., Driscoll, C.T., Fahey, T.J., Siccama, T.G., 2001. Plant-soil-microbial interactions in a northern hardwood forest. Ecology 82, 965–978.

Booth, M.S., Stark, J.M., Rastetter, E.B., 2005. Controls on nitrogen cycling in terrestrial ecosystems: a synthetic analysis of literature data. Ecological Monographs 75, 139–157.

Brooks, P.D., Stark, J.M., McInteer, B.B., Preston, T., 1989. Diffusion method to prepare soil extracts for automated N-15 analysis. Soil Science Society of America Journal 53, 1707–1711.

Brown, J.W., 1958. Forest history of Mount Moosilauke, Part II: big logging days andn their aftermath (1890-1940). Appalachia 24, 221–233.

Burns, R.G., 1982. Enzyme activity in soil: location and a possible role in microbial ecology. Soil Biology and Biochemistry 14, 423–427.

Carreiro, J.E., Walter, C.A., Hawkins, J.S., Peterjohn, W.T., Averill, C., Brzostek, E.R., 2018. Interactions among plants, bacteria, and fungi reduce extracellular enzyme activities under long-term N fertilization. Global Change Biology 24, 2721–2734.

Christenson, L.M., Lovett, G.M., Weathers, K.C., Arthur, M.A., 2009. The influence of tree species, nitrogen fertilization, and soil C to N ratio on gross soil nitrogen transformations. Soil Science Society of America Journal 73, 638–646.

Compton, J.E., Hooker, T.D., Perakis, S.S., 2007. Ecosystem N distribution and δ^{15}N during a century of forest regrowth after agricultural abandonment. Ecosystems 10, 1197–1208.

Davidson, E.A., Hart, S.C., Shanks, C.A., Firestone, M.K., 1991. Measuring gross nitrogen mineralization, immobilization, and nitrification by ^{15}N isotopic pool dilution in intact soil cores. Journal of Soil Science 42, 335–349.

DeForest, J.L., 2009. The influence of time, soil temperature, and substrate age on potential soil enzyme activity in acidic forest soils using MUB-linked substrates and L-DOPA. Soil Biology and Biochemistry 56, 263–270.

Ekenler, M., Tabatabai, M.A., 2002. Beta-glucosaminidase activity of soils: effect of cropping systems and its relationship to nitrogen mineralization. Biology and Fertility of Soils 36, 367–376.

Fahey, T.J., Siccama, T.G., Driscoll, C.T., Likens, G.E., Campbell, J., Johnson, C.E., Battles, J.J., Aber, J.D., Cole, J.J., Fisk, M.C., Groffman, P.M., Hamburg, S.P., Holmes, R.T., Schwarz, P.A., Yanai, R.D., 2005. The biogeochemistry of carbon at Hubbard Brook. Biogeochemistry 75, 109–176.

Fatemi, F.R., Fernandez, I.J., Simon, K.S., Dail, D.B., 2016. Nitrogen and phosphorus regulation of soil enzyme activities in acid forest soils. Soil Biology and Biochemistry 98, 171–179.

Federer, C.A., 1983. Nitrogen mineralization and nitrification: depth variation in four New England forest soils. Soil Science Society of America Journal 47, 1008–1014.

Fierer, N., Schimel, J.P., Cates, R.G., Zou, J., 2001. Influence of balsam popular tannin fractions on carbon and nitrogen dynamics in Alaskan taiga floodplain soils. Soil Biology and Biochemistry 33, 1827–1839.

Fierer, N., Schimel, J.P., Holden, P.A., 2003. Variations in microbial community composition through two soil depth profiles. Soil Biology and Biochemistry 35, 167–176.

Fisk, M.C., Zak, D.R., Crow, T.R., 2002. Nitrogen storage and cycling in old- and second-growth northern hardwood forests. Ecology 83, 73–87.

Frey, S.D., 2019. Mycorrhizal fungi as mediators of soil organic matter dynamics. Annual Review of Ecology Evolution and Systematics 50, 237–259.

Frey, S.D., Knorr, M., Parrent, J.L., Simpson, R.T., 2004. Chronic nitrogen enrichment affects the structure and function of the soil microbial community in temperate hardwood and pine forests. Forest Ecology and Management 196, 159–171.

Fuss, C.B., Lovett, G.M., Goodale, C.L., Ollinger, S.V., Lang, A.K., Ouimette, A.P., 2019. Retention of nitrate-N in mineral soil organic matter depends on forest age. Ecosystems 22 (6), 1280–1294.

Gaudinski, J., Trumbore, S., Davidson, E.A., 2000. Soil carbon cycling in a temperate forest: radiocarbon-based estimates of residence times. Biogeochemistry 51, 33–69.

German, D.P., Weintraub, M.N., Grandy, A.S., Lauber, C.L., Rinkes, Z.L., Allison, S.D., 2011. Optimization of hydrolytic and oxidative enzyme methods for ecosystem studies. Soil Biology and Biochemistry 43, 1387–1397.

Goodale, C.L., Aber, J.D., Vitousek, P.M., 2003. An unexpected nitrate decline in New Hampshire streams. Ecosystems 6, 75–86.

Groffman, P.M., Fisk, M.C., Driscoll, C.T., Likens, G.E., Fahey, T.J., Eagar, C., Pardo, L.H., 2006. Calcium additions and microbial nitrogen processes in a northern hardwood forest. Ecosystems 9, 1289–1305.

Groffman, P.M., Driscoll, C.T., Duran, J., Campbell, J.L., Christenson, L.M., Fahey, T.J., Fisk, M.C., Fuss, C., Likens, G.E., Lovett, G., Rustad, L., Templer, P.H., 2018. Nitrogen oligotrophication in northern hardwood forests. Biogeochemistry. https://doi.org/10.1007/s10533-018-0445-y.

Hart, S.C., Nason, G.E., Myrold, D.D., Perry, D.A., 1994. Dynamics of gross nitrogen transformations in an old-growth forest: the carbon connection. Ecology 75, 880–891.

Herold, N., Schöning, I., Berner, D., Haslwimmer, H., Kandeler, E., Michalzik, B., Schrumpf, M., 2014. Vertical gradients of potential enzyme activities in soil profiles of European beech, Norway spruce and Scots pine dominated forest sites. Pedobiologia 1–9.

Hicks Pries, C.E., Castanha, C., Porras, R.C., Torn, M.S., 2017. The whole-soil carbon flux in response to warming. Science 355, 1420–1423.

Hobbie, J., Hobbie, E., 2006. ^{15}N in symbiotic fungi and plants estimates nitrogen and carbon flux rates in Arctic tundra. Ecology 87, 816–822.

Högberg, P., 1997. Tansley Review No. 95: ^{15}N natural abundance in soil-plant systems. New Phytologist 137, 179–203.

Iversen, C.M., Hooker, T.D., Classen, A.T., Norby, R.J., 2011. Net mineralization of N at deeper soil depths as a potential mechanism for sustained forest production under elevated $[CO_2]$. Global Change Biology 17, 1130–1139.

Jobbagy, E.G., Jackson, R.B., 2001. The distribution of soils nutrients with depth: global patterns and the imprint of plants. Biogeochemistry 53, 51–77.

Johnson, C.E., 1995. Soil nitrogen status 8 years after whole tree clear cutting. Canadian Journal of Forest Research 25, 1346–1355.

Johnson, D.W., 1992. Nitrogen retention in forest soils. Journal of Environmental Quality 21, 1–12.

Kaye, J.P., Binkley, D., Rhoades, C., 2003. Stable soil nitrogen accumulation and flexible organic matter stoichiometry during primary floodplain succession. Biogeochemistry 63, 1–22.

Keiluweit, M., Bougoure, J.J., Nico, P.S., Pett-Ridge, J., Weber, P.K., Kleber, M., 2015. Mineral protection of soil carbon counteracted by root exudates. Nature Climate Change 5, 588–595.

Kellman, L., Kumar, S., Diochon, A., 2014. Soil nitrogen dynamics within profiles of a managed moist temperate forest chronosequence consistent with long-term harvesting-induced losses. JGR-Biogeosciences 119, 1309–1321.

Keurajian, A., 2015. Nitrogen Accumulation in Woody Biomass of *Betula Alleghaniensis* and *Acer Saccharum* on Mount Moosilauke Old Growth Forest. Cornell University Department of Ecology and Evolutionary Biology Undergraduate Honors Thesis.

Kirkham, D., Bartholomew, W.V., 1955. Equations for following nutrient transformations in soil, utilizing tracer data. Soil Science Society of America Proceedings 19, 189–192.

Koven, C.D., Riley, W.J., Subin, Z.M., Tang, J.Y., Torn, M.S., Collins, W.D., Bonan, G.B., Lawrence, D.M., Swenson, S.C., 2013. The effect of vertically resolved soil biogeochemistry and alternate soil C and N models on C dynamics of CLM4. Biogeosciences 10, 7109–7131.

Kramer, M.G., Lajtha, K., Aufdenkampe, A., 2017. Depth trends of soil organic matter C:N and ^{15}N natural abundance controlled by association with minerals. Biogeochemistry 136 (3), 237–248.

Kuzyakov, Y., 2010. Priming effects: interactions between living and dead organic matter. Soil Biology and Biochemistry 42, 1363–1371.

Kuzyakov, Y., Friedel, J.K., Stahr, K., 2000. Review of mechanisms and quantification of priming effects. Soil Biology and Biochemistry 32, 1485–1498.

Likens, G.E., 2013. Biogeochemistry of a Forested Ecosystem. Springer-Verlag, New York.

Ladd, J.N., 1978. Origin and range of enzymes in soil. In: Burns, R.G. (Ed.), Soil Enzymes. Academic Press, London, pp. 51–96.

Lee, Y.B., Lorenz, N., Dick, L.K., Dick, R.P., 2007. Cold storage and pretreatment incubation effects on soil microbial properties. Soil Science Society of America Journal 71 (4), 1299–1305.

Looby, C.I., Treseder, K.K., 2018. Shifts in soil fungi and extracellular enzyme activity with simulated climate change in a topical montane cloud forest. Soil Biology and Biochemistry 117, 87–96.

Lovett, G.M., Goodale, C.L., Ollinger, S.V., Fuss, C.B., Ouimette, A.P., Likens, G.E., 2018. Nutrient retention during ecosystem succession: a revised conceptual model. Frontiers in Ecology and the Environment 16 (9), 1–7. https://doi.org/10.1002/fee.1929.

Matejek, B., Huber, C., Dannenmann, M., Kohlpaintner, M., Gasche, R., Göttlein, A., Papen, H., 2010. Microbial nitrogen turnover processes within the soil profile of a nitrogen saturated spruce forest and their relation to the small-scale pattern of seepage-water nitrate. Journal of Plant Nutrition and Soil Science 173, 224–236.

McFarlane, K.J., Torn, M.S., Hanson, P.J., Porras, R.C., Swanston, C., Callaham, M.A., Guilderson, T.P., 2013. Comparison of soil organic matter dynamics at five temperate deciduous forests with physical fractionation and radiocarbon measurements. Biogeochemistry 112, 457–476.

Meier, I.C., Finzi, A.C., Phillips, R.P., 2017. Root exudates increase N availability by stimulating microbial turnover of fast-cycling N pools. Soil Biology and Biochemistry 106, 119–128.

Moorhead, D.L., Sinsabaugh, R.L., 2006. A theoretical model of litter decay and microbial interaction. Ecological Monographs 76, 151–174.

Moorhead, D.L., Sinsabaugh, R.L., Hill, B.H., Weintraub, M.N., 2016. Vector analysis of ecoenzyme activities reveal constraints on coupled C, N, and P dynamics. Soil Biology and Biochemistry 93, 1–7.

Mooshammer, M., Wanek, W., Zechmeisgter-Boltenstern, S., Richter, A., 2014. Stoichiometric imbalances between terrestrial decomposer communities and their resources: mechanisms, and implications of microbial adaptations to their resources. Frontiers in Microbiology 5 (22), 1–10.

Morse, J.L., Werner, S.F., Gillin, C.P., Goodale, C.L., Bailey, S.W., McGuire, K.J., Groffman, P.M., 2014. Searching for biogeochemical hot spots in three dimensions: soil C and N cycling in hydropedologic settings in a northern hardwood forest. Journal of Geophysical Research: Biogeosciences 119, 1596–1607.

Peart, D.R., Cogbill, C.V., Palmiotto, P.A., 1992. Effects of logging history and hurricane damage on canopy structure in a northern hardwoosd forest. Bulletin of the Torrey Botanical Club 119, 29–38.

Persson, T., Wirén, A., 1995. Nitrogen mineralization and potential nitrification at different depths in acid forest soils. Plant and Soil 168–169, 55–65.

Phillips, R.P., Meier, I.C., Bernhardt, E.S., Grandy, A.S., Wickings, K., Finzi, A.C., 2012. Roots and fungi accelerate carbon and nitrogen cycling in forests exposed to elevated CO_2. Ecology Letters 15, 1042e1049.

Porras, R.C., Hicks Pries, C.E., McFarlane, K.J., Hanson, P.J., Torn, M.S., 2017. Association with pedogenic iron and aluminum: effects on soil organic carbon storage and stability in four temperate forest soils. Biogeochemistry 133, 333–345.

Rau, B.M., Melvin, A.M., Johnson, D.W., Goodale, C.L., Blank, R.R., Fredriksen, G., Miller, W.W., Murphy, J.D., Todd, D.E., Walker, R.F., 2011. Revisiting soil carbon and nitrogen sampling: quantitative pits versus rotary cores. Soil Science 176, 273–279.

Richter, D.D., Markewitz, D., Heine, P.R., Jin, V., Raikes, J., Tian, K., Wells, C.G., 2000. Legacies of agriculture and forest regrowth in the nitrogen of old-field soils. Forest Ecology and Management 138, 233–248.

Riggs, C.E., Hobbie, S.E., 2016. Mechanisms driving the soil organic matter decomposition response to nitrogen enrichment in grassland soils. Soil Biology and Biochemistry 99, 54–65.

Robertson, G.P., Wedin, D., Groffman, P.M., Blair, J.M., Holland, E.A., Nadelhoffer, K.J., Harris, D., 1999. Soil carbon and nitrogen availability: nitrogen mineralization, nitrification, and soil respiration potentials. In: Robertson, G.P., Coleman, D.C., Bledsoe, C.S., Sollins, P. (Eds.), Standard Soil Methods for Long-Term Ecological Research. Oxford University Press, pp. 258–271.

Rumpel, C., Kögel-Knabner, I., 2011. Deep soil organic matter – a key but poorly understood component of terrestrial C cycle. Plant and Soil 338, 143–158.

Schimel, J.P., Bennett, J., 2004. Nitrogen mineralization: challenges of a changing paradigm. Ecology 85, 591–602.

Schleppi, P., Bucher-Wallin, I., Hagedorn, F., Korner, C., 2012. Increased nitrate availability in the soil of a mixed mature temperate forest subjected to elevated CO_2 concentration (canopy FACE). Global Change Biology 18, 757–768.

Schmidt, M.W.I., Torn, M.S., Abiven, S., Dittmar, T., Guggenberger, G., Janssens, I.A., Kleber, M., Kögel-Knabner, I., Lehmann, J., Manning, D.A.C., Nannipieri, P., Rasse, D.P., Weiner, S., Trumbore, S.E., 2011. Persistence of soil organic matter as an ecosystem property. Nature 478, 49.

Schrumpf, M., Kaiser, K., Guggenberger, G., Persson, T., Kogel-Knaber, I., Schulze, E.-D., 2013. Storage and stability of organic carbon in soils as related to depth, occlusion within aggregates, and attachment to minerals. Biogeosciences 10, 1675–1691.

Sinsabaugh, R.L., 2010. Phenol oxidase, peroxidase and organic matter dynamics of soil. Soil Biology and Biochemistry 42, 391–404.

Sinsabaugh, R.L., Moorhead, D.L., 1994. Resource allocation to extracellular enzyme production: a model for nitrogen and phosphorus control of litter decomposition. Soil Biology and Biochemistry 26 (10), 1305–1311.

Sinsabaugh, R.L., Follstad Shah, J.J., 2011. Ecoenzymatic stoichiometry of recalcitrant organic matter decomposition: the growth rate hypothesis in reverse. Biogeochemistry 102, 31–43.

Sinsabaugh, R.L., Carreiro, M.M., Repert, D.A., 2002. Allocation of extracellular enzymatic ativity in relation to litter composition, N deposition, and mass loss. Biogeochemistry 60, 1–24.

Sinsabaugh, R.L., Gallo, M.E., Lauber, C., Waldrop, M.P., Zak, D.R., 2005. Extracellular enzyme activities and soil organic matter dynamics for northern hardwood forests receiving simulated nitrogen deposition. Biogeochemistry 75 (2), 201–215.

Sinsabaugh, R.L., Lauber, C.L., Weintraub, M.N., Ahmed, B., Allison, S.D., Crenshaw, C., Contosta, A.R., Cusack, D., Frey, S., Gallo, M.E., Gartner, T.B., Hobbie, S.E., Holland, K., Keeler, B.L., Powers, J.S., Stursova, M., Takacs-Vesbach, C., Waldrop, M.P., Wallenstein, M.D., Zak, D.R., Zeglin, L.H., 2008. Stoichiometry of enzyme activity at global scale. Ecology Letters 11, 1252–1264.

Sinsabaugh, R.L., Hill, B.H., Follstad Shah, J.J., 2009. Ecoenzymatic stoichiometry of microbial organic nutrient acquisition in soil and sediment. Nature 462, 795–798.

Sollins, P., Kramer, M.G., Swanston, C., Lajtha, K., Filley, T., Aufdenkampe, A.K., Wagai, R., Bowden, R.D., 2009. Sequential density fractionation across soils of contrasting mineralogy: evidence for both microbial- and mineral-controlled soil organic matter stabilization. Biogeochemistry 96, 209–231.

Stone, M.M., Plante, A.F., 2014. Changes in phosphatase kinetics with soil depth across a variable tropical landscape. Soil Biology and Biochemistry 71, 61–67.

Stone, M.M., Plante, A.F., 2015. Relating biological stability of soil organic matter to energy availability in deep tropical soil profiles. Soil Biology and Biochemistry 89, 162–171.

Stone, M.M., DeForest, J.L., Plante, A.F., 2014. Changes in extracellular enzyme activity and microbial community structure with soil depth at the Luquillo Critical Zone Observatory. Soil Biology and Biochemistry 75, 237–247.

Stone, M.M., Kan, J., Plante, A.F., 2015. Parent material and vegetation influence bacterial community structure and nitrogen functional genes along deep tropical soil profiles at the Luquillo Critical Zone Observatory. Soil Biology and Biochemistry 80, 273–282.

Tabatabai, M.A., Ekenler, M., Senwo, Z.N., 2010. Significance of enzyme activities in soil nitrogen mineralization. Communications in Soil Science and Plant Analysis 41 (5), 595–605.

Talbot, J.M., Allison, S.D., Treseder, K.K., 2008. Decomposers in disguise: mycorrhizal fungi as regulators of soil C dynamics in ecosystems under global change. Functional Ecology 22, 955–963.

Taylor, J., Wilson, B., Mills, M., Burns, R.G., 2002. Comparison of microbial numbers and enzymatic activities in surface soils and subsoils using various techniques. Soil Biology and Biochemistry 34, 387–401.

Vitousek, P.M., Reiners, W.A., 1975. Ecosystem succession and nutrient retention: a hypothesis. BioScience 25, 376–381.

Wallenius, K.H., Rita, H., Simpanen, S., Mikkonen, A., Niemi, R.M., 2010. Sample storage for soil enzyme activity and bacterial community profiles. Journal of Microbiological Methods 81 (1), 48–55.

Weand, M.P., Arthur, M.A., Lovett, G.M., McCulley, R.L., Weathers, K.C., 2010. Effects of tree species and N additions on forest floor microbial communities and extracellular enzyme activities. Soil Biology and Biochemistry 42, 2161–2173.

Weintraub, M.N., Scott-Denton, L.E., Schmidt, S.E., Monson, R.K., 2007. The effects of tree rhizodeposition on soil exoenzyme activity, dissolved organic carbon, and nutrient availability in a subalpine forest ecosystem. Oecologia 154, 327–338.

Wieder, W.R., Bonan, G.B., Allison, S.D., 2013. Global soil carbon projections are improved by modelling microbial processes. Nature Climate Change 3 (10), 909–912.

Wieder, W.R., Allison, S.D., Davidson, E.A., Georgiou, K., Hararuk, O., He, Y., Hopkins, F., Luo, Y., Smith, M.J., Sulman, B., Todd-Brown, K., Wang, Y.-P., Xia, J., Xu, X., 2015. Explicitly representing soil microbial processes in Earth system models. Global Biogeochemical Cycles 29, 1782–1800.

Yuan, Y., Zhao, W., Zhang, Z., Xiao, J., Li, D., Liu, Q., Yin, H., 2018. Impacts of oxalic acid and glucose additions on N transformation in microcosms via artificial roots. Soil Biology and Biochemistry 121, 16–23.

Zaman, M., Di, H.J., Cameron, K.C., Frampton, C.M., 1999. Gross nitrogen mineralization and nitrification rates and their relationships to enzyme activities and the soil microbial biomass in soils treated with dairy shed effluent and ammonium fertilizer at different water potentials. Biology and Fertility of Soils 29, 178–186.

Zechmeister-Boltenstern, S., Keiblinger, K.M., Mooshammer, M., Penuelas, J., Richter, A., Sardans, J., Wanek, W., 2015. The application of ecological stoichiometry to plant-microbial-soil organic matter transformations. Ecological Monographs 85 (2), 133–155.